Memory effects in active droplets

Quynh Nhu T. Le[a†], Kueyoung E. Kim[a†], Bryan Kaehr [b], Lauren D. Zarzar[a,c,d*]

[a] Department of Chemistry, The Pennsylvania State University, University Park, PA 16802, USA
[b] Advanced Materials Laboratory, Sandia National Laboratories, Albuquerque, NM 87185, USA
[c] Department of Materials Science and Engineering, The Pennsylvania State University, University Park, PA 16802, USA
[d] Materials Research Institute, The Pennsylvania State University, University Park, PA 16802, USA

[†] Authors contributed equally to this work
*Corresponding author

Abstract

Marangoni-driven self-propelled droplets have attracted considerable attention as a platform to study active soft matter and collective behavior. The speed of active drops is generally assumed to be determined by instantaneous diameter and solubilization rate, which together dictate the spontaneously generated interfacial tension gradients across the drop surface and induce propulsion; the history of the droplet has not before been considered. Here, we report that active droplets can exhibit a type of memory wherein the temporal history of the droplet, particularly the starting diameter, influences the droplet speed. For example, two droplets of identical instantaneous diameter in the same local chemical environment can exhibit dramatically different instantaneous velocities depending upon their initial diameter. This effect is observed for a range of droplet oils and common ionic surfactants. The relationships between drop diameter, velocity, and solubilization rate were examined for several ionic and nonionic surfactants and suggest that droplet motility only is present when solubilization is interfacially limited, as opposed to diffusion limited. Oil droplets in ionic surfactant solutions also undergo a transition from motile to non-motile, where the diameter at the transitionary point depends upon initial drop diameter. We hypothesize that this memory behavior may result from an interfacial phase transition, as hinted at by observed visual deformations on drop interfaces under some circumstances. We believe this work provides insight as to how memory may be imparted in active droplet systems, highlights the importance of non-equilibrium phenomena in active materials, and offers valuable insights for the design of adaptive, dynamic droplet systems.

Introduction

Emerging from the study of nonequilibrium systems, active colloids have become a pivotal topic in fundamental soft matter research, fueling breakthroughs in biomimetic materials,[1–3] life-like droplets,[4–6] and the understanding of far-from-equilibrium phenomena. Among such active colloids, motile droplets have drawn significant interest for their simple composition and ease of fabrication, yet rich dynamics.[7] These emulsions consist of a minimum of one immiscible liquid dispersed in another, with a surfactant acting as a stabilizer. Droplets self-propel and communicate with each other via chemical gradients that spontaneously generate interfacial tension gradients and Marangoni flows on the drop surfaces.[8–10] While chemical reactions can be used to induce drop self-propulsion, the simplest systems are fueled only by solubilization processes wherein droplet contents are transferred into the surrounding solution; spontaneous symmetry breaking coupled with a positive feedback mechanism can lead to sustained droplet motility in the absence of any other applied fields or forces.[11–13] Despite the widespread study of solubilizing active droplets with diverse chemistries[9,14–16] and various models proposed to rationalize their active behaviors[10,15,17], a molecular-level understanding of how solute transport at a non-equilibrium oil–

water interface generates interfacial tension gradients and thus self-propulsion remains elusive. Notably, although active droplets have non-equilibrium interfaces, drop motility has always been described as a function of instantaneous properties such as diameter,[18,19] i.e. independent of their history and initial condition.[19] This approach may not fully capture droplet properties since non-equilibrium soft materials frequently exhibit memory effects.[20] A material at equilibrium—such as a perfect crystal—will always have the same properties regardless of its history, while a non-equilibrium system—such as a soft glassy material (foams, emulsions, pastes, slurries)—can display strong dependence on its past.[21,22]

Here, we report that solubilizing active droplets can exhibit history-dependent motility. This memory effect manifests in unexpected changes in a droplet's velocity, which at any point in time might be dependent not only on its instantaneous diameter, but also on a diameter from earlier in the droplet's life. For instance, we observe two drops of identical composition and size in the same chemical environment swimming at dramatically different speeds depending on their initial diameters (i.e. diameter at which the drop was formed). Tracking the velocity of active droplets across a diverse range of surfactant types, we find that this memory effect is linked to solubilization kinetics: only active, motile droplets with non-constant solubilization rates are history-dependent. We hypothesize that a slow, interfacial phase transition might impact the solubilization rates of some active drops. We hope that this work contributes fundamental insights into principles governing active droplet behavior, facilitates the design of emergent behaviors in active matter, and spark further investigations surrounding non-equilibrium interfacial processes in emulsions.

Results and Discussion

Self-propelled active droplets irreversibly stop at different diameters. Our discovery of history-dependent active droplets occurred while observing a single, 1-bromooctane droplet with an initial diameter of $D_0 \approx 100$ µm in 5 wt% aqueous sodium dodecyl sulfate (SDS, CMC = 0.2 wt%). The droplet was confined in a submerged, circular corral (1 mm diameter and 0.2 mm depth with an open top) to keep the droplet in the field of view as it actively self-propelled due to micellar solubilization of the oil. Although the drop was initially highly active with instantaneous velocity, V, exceeding 200 µm/s, the droplet gradually slowed and came to a halt after about 18 minutes, despite continuing to solubilize (**Fig. 1A, Video S1**). This stopping behavior was also observed with *n*-octane. Particle image velocimetry of the droplet side-profile revealed zero interfacial flow when the droplet stopped (**Fig. 1B, Video S2**). Agitation of the solution to refresh the droplet's local environment, or transfer of the stopped droplet to a dish with fresh SDS solution, did not restart motion, indicating that a local buildup of oil-filled micelles was not causing the loss of motility.

On one hand, it is expected that droplet motility should decrease with drop diameter due to a decrease in Péclet number (Pe), which compares advective to diffusive transport: $Pe = \mathcal{A}\mathcal{M}D/\mathcal{D}^2$, where $\mathcal{A}$, $\mathcal{M}$, and D are the drop's activity, mobility, and diameter, and $\mathcal{D}$ is the diffusivity of a filled micelle. As such, we considered that perhaps the droplet simply became too small to sustain self-propulsion.[15,19,23] However, a second, freshly emulsified droplet of equivalent diameter to that of the first, stopped droplet ($D_0 \approx 46$ µm) added to the same corral was quite active (**Fig. 1C**). The second droplet eventually stopped moving as well, but its diameter upon halting was much smaller than the first drop (23 µm vs 38 µm). These observations suggested that there are factors independent of the instantaneous droplet diameter and local chemical environment that affect motility, and it appeared that the droplet's history, i.e. starting diameter, could be playing a role.

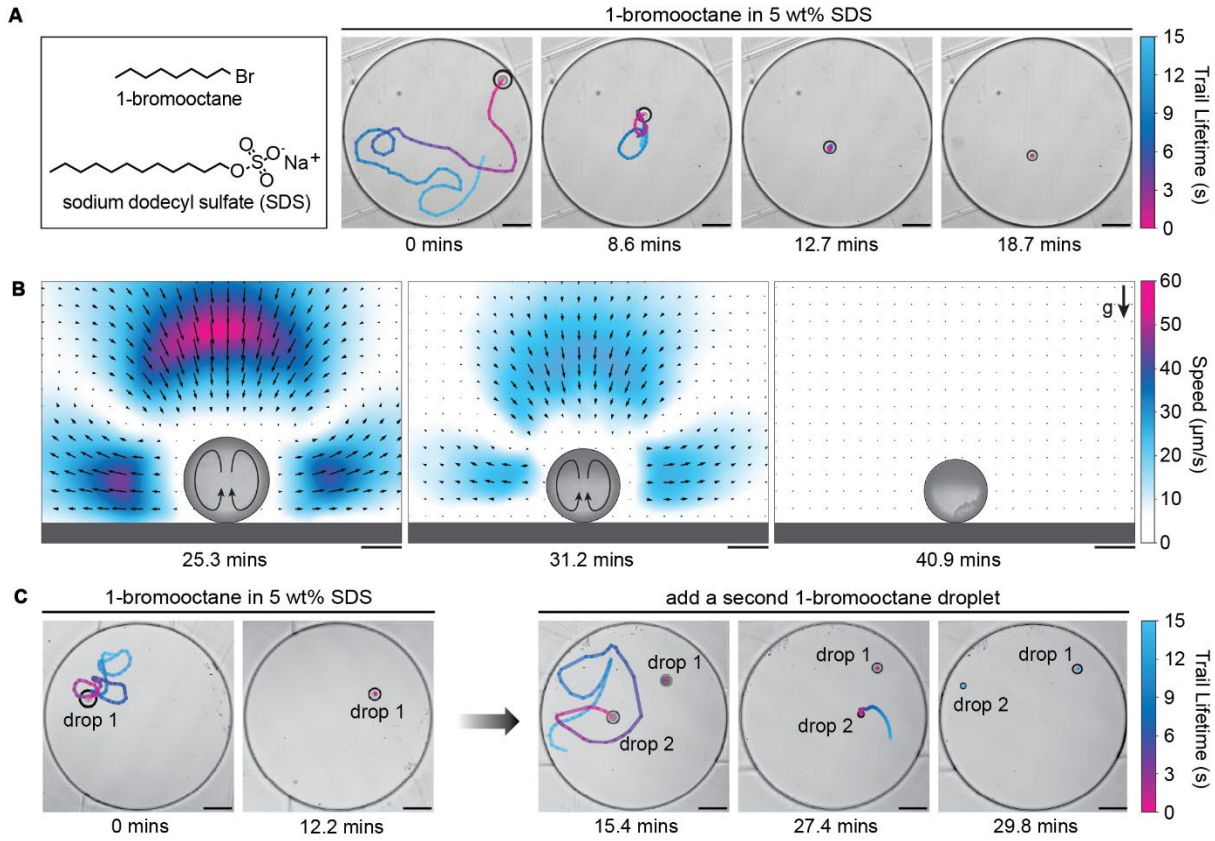

Figure 1. **A self-propelled 1-bromooctane drop in SDS solution stops irreversibly. (A)** A 1-bromooctane drop with initial diameter D_0 ≈ 100 μm in aqueous 5 wt% SDS solution is initially highly motile. Over time, the droplet slows down and eventually stops moving. Agitation of the solution does not restart drop motion. Scale, 100 μm. **(B)** Experimental flow fields around the side profile of a 1-bromooctane droplet in 5 wt% SDS captured using particle image velocimetry. Over time, the velocity of the surrounding flow decreases until it ceases completely, which is associated with the loss in droplet motility. Note that flow should be fastest close to the droplet interface; however, we were unable to record accurate flow velocities at those locations due to low particle number densities directly adjacent to the drop's interface. Scale, 50 μm. **(C)** After allowing a D_0 ≈ 100 μm 1-bromooctane drop in 5 wt% SDS to stop (drop 1) at a diameter of D ≈ 46 μm, a second size-matched, freshly emulsified 1-bromooctane droplet was added to the same dish (drop 2). Drop 2 was active initially, but eventually stopped moving over time, albeit at a much smaller diameter than drop 1. This result indicates that stopping is not due to reaching critical diameter. Scale, 100 μm.

Stopping diameter depends on droplet initial diameter. For a range of D_0, we measured the stopping diameter, defined as the diameter at which the flow around the drop's side profile ceased. We observed a strong positive correlation (**Fig. 2A**), demonstrating droplet memory of their initial condition. Seeking a more detailed understanding of how these drops evolved over their lifetimes, we tracked the diameters and velocities of 1-bromooctane drops with D_0 = 50, 75, and 100 μm in 5 wt% SDS solution (**Fig. 2B**). All drops gradually slowed down until they reached a lateral velocity of V = 0 μm/s but still continued to solubilize and decrease in diameter afterwards. Examining the trends in $V(t)$ and $D(t)$, we noticed that

the solubilization rate (κ), defined as the change in drop diameter with respect to time, $\kappa = \left|\frac{dD}{dt}\right|$, underwent a transition around the same time that droplets reached V = 0 µm/s (**Fig. 2B**). For a given chemistry (oil and surfactant), we typically expect that an active drop's velocity is determined by its instantaneous diameter and solubilization rate, i.e. $V = V(D, \kappa)$.[11] To visualize the connection between these variables, we re-plotted the trajectory data for the 1-bromooctane drops in 5 wt% SDS from **Fig. 2B** to include κ as a parameter (**Fig. 2C**). Each drop traversed unique paths in (D, κ, V) space that, surprisingly, depended on D_0. To check whether this behavior was unique to SDS, we also conducted the same experiment using 1-bromooctane drops in 3 wt% of the cationic surfactant tetradecyltrimethylammonium bromide (TTAB; **Fig. S1**). Notably, despite differences in their molecular structures, SDS and TTAB were functionally identical in terms of the relationship between drop motility and solubilization.

Examining **Fig. 2C** more closely hints at the importance of κ to droplet memory. In **Fig. 2C**, we see that drop behavior could be divided into three regimes: an inactive regime at smaller diameters, an active regime at larger diameters, and a transitionary regime in between. Within the inactive regime, κ increased as drops got smaller, implying diffusion-limited solubilization; i.e., diffusion of oil-filled micelles away from the drop is slow relative to oil dissolution into the water, so smaller droplets enable faster solubilization.[24] Noting that the κ vs D curves roughly aligned for drops with different D_0 within the inactive regime, we conclude that the solubilization rate of non-motile drops is determined by their instantaneous D. Within the active regime, initially, κ was fairly constant. However, during the transition from active to inactive, κ decreased, manifesting in a reduced V. Interestingly, the diameter range at which this transitionary regime occurred was dependent on D_0; larger D_0 drops transition at larger diameters. As such, droplets with the same D could have dramatically different κ depending on D_0—just as drop motility was observed to depend on D_0.

To rationalize the halting behavior, we looked at the relationship between D, κ, and V, which can be described by the Péclet number, Pe. Pe is a function of D and κ and determines droplet velocity, i.e. $V = V(Pe)$.[8,11,25] Additionally, self-propulsion is expected only above a critical Péclet number, $Pe_c = 4$.[25] As such, we suspected that our drops were slowing down and stopping due to a low Pe caused by the coupled, simultaneous decrease in D and κ observed in **Fig. 2C**. We set out to estimate the time evolution of Péclet number for our experiments. Following the analysis presented by Izri *et al.* to calculate Pe for solubilizing active droplets (see "Calculation of Péclet number for active droplets" in SI for details),[11] we estimated the instantaneous Péclet number for the 1-bromooctane drops in 5 wt% SDS (**Fig. 2D**) and 3 wt% TTAB (**Fig. S1**). We found that V was well described by the estimated Pe for all drops regardless of D_0. Additionally, all drops stopped for Péclet numbers within an order-of-magnitude of the theoretically expected value of $Pe_c = 4$. Thus, we conclude that the irreversible stopping of 1-bromooctane drops in SDS and TTAB is likely caused by a low Pe, which in turn is due to the drop's decreasing D and κ.

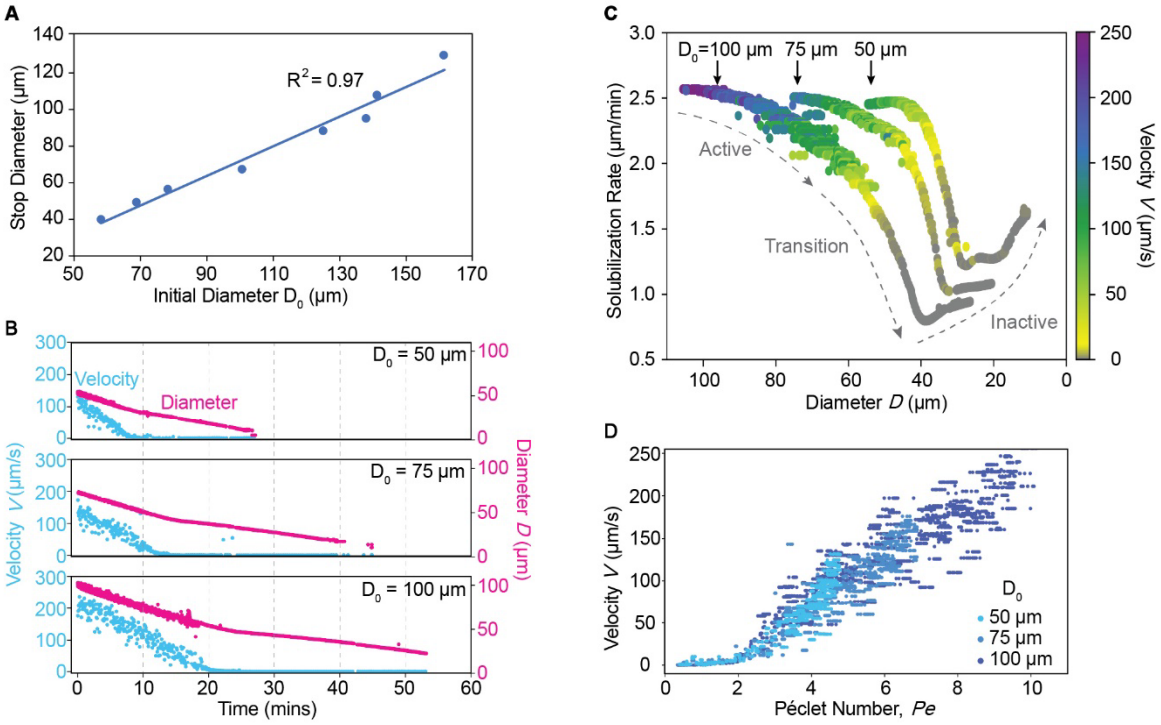

Figure 2. Motility of 1-bromooctane in SDS is dependent on initial diameter. (A) Stopping vs initial diameters for 1-bromooctane drops in 5 wt% aqueous SDS. The stopping diameter was determined based on the time at which tracer particle flow around the drop ceased. Linear regression between initial and stopping diameters yielded an R^2 value of 0.97. **(B)** Time evolution of velocity (blue) and diameter (pink) for 1-bromooctane drops with varying D_0 in 5 wt% SDS. **(C)** Velocity as a function of drop diameter and solubilization rate for 1-bromooctane drops with varying D_0 in 5 wt% SDS. **(D)** Velocity of drops with varying D_0 as a function of Péclet number for 1-bromooctane drops in 5 wt% SDS. Data in (B–D) are from the same set of experiments. Representative single droplet trajectories are plotted for clarity; experiments were performed in triplicate and additional data is reported in **Fig. S3**.

Droplet "memory" arises from a dependence of κ upon D_0. To try to gain additional insight regarding how κ depends upon D_0 and relates to droplet memory, we decided to explore active droplets in different chemical systems, especially those containing nonionic surfactants. We tracked the solubilization kinetics and velocities of 1-bromooctane drops with varying D_0 in aqueous 2 wt% Tergitol NP-9 (**Fig. 3A**) and 5 wt% Makon TD-12 (**Fig. S2**). Tergitol NP-9 is a nonylphenol ethoxylate surfactant (CMC = 0.006 wt%) and Makon TD-12 is an alkyl ethoxylate (CMC = 0.013 wt%). Similar to 1-bromooctane in SDS, larger drops were faster, and velocities decreased over time in both surfactants (**Fig. 3B**). However, none of the drops in these nonionic surfactants stopped moving. Drops remained active until they were no longer visible under the microscope. The solubilization kinetics were also different than in SDS and TTAB; κ was constant throughout a drop's lifetime (**Fig. 3C**) which is similar to other reports of active drops in nonionic surfactants.[14,26,27] Plotting V vs D (**Fig. 3D**), we found that drop velocity was the same for a given D regardless of D_0, i.e. not history dependent. The fact that both the history dependent behavior and solubilization kinetics of 1-bromooctane differed between SDS/TTAB (ionic surfactants) and Tergitol NP-9/Makon TD-12 (nonionic surfactants) made us suspect that the temporal evolution of κ depending on D_0 could underpin droplet memory and that it has some physical basis in the drop surface chemistry.

The velocity of an active solubilizing droplet has been proposed to scale as:[11]

$$V(t) \propto \kappa(t) D(t) \tag{1}$$

This relation suggests that history dependence—that is, dependence of V on D_0—should emerge from $\kappa(t)$ and/or $D(t)$. We consider how a single oil droplet evolves over time within this framework. A solubilizing drop will start at (D_0, κ_0) and traverse a path through (D, κ) space over its lifetime. This trajectory corresponds to the time evolution of the velocity. If κ is constant, all drops will follow the same path through (D, κ) space regardless of D_0, meaning their initial condition (D_0, κ_0) is not important to their lifetime dynamics and thus are history independent with no memory of their starting condition (**Fig. 3C, Fig. S2**). However, for non-constant κ, different D_0 values generate unique trajectories through (D, κ) space and thus would be expected to lead to history dependence (e.g. **Fig. 2C, Fig. S1**). (Note that there is also a non-constant increasing κ in the inactive regime where velocity is zero, which arises due to diffusion limitations, and is not the focus here). The importance of non-constant decreasing κ in determining active drop history dependence can be demonstrated mathematically—the expression for V should depend explicitly on D_0 in this case (see "Non-constant solubilization rates cause initial diameter dependence" in the supporting information). Thus, the non-constant (decreasing) κ within the active regime imparts the droplet with memory of its starting diameter, which manifests as these unexpected changes in the droplet motility.

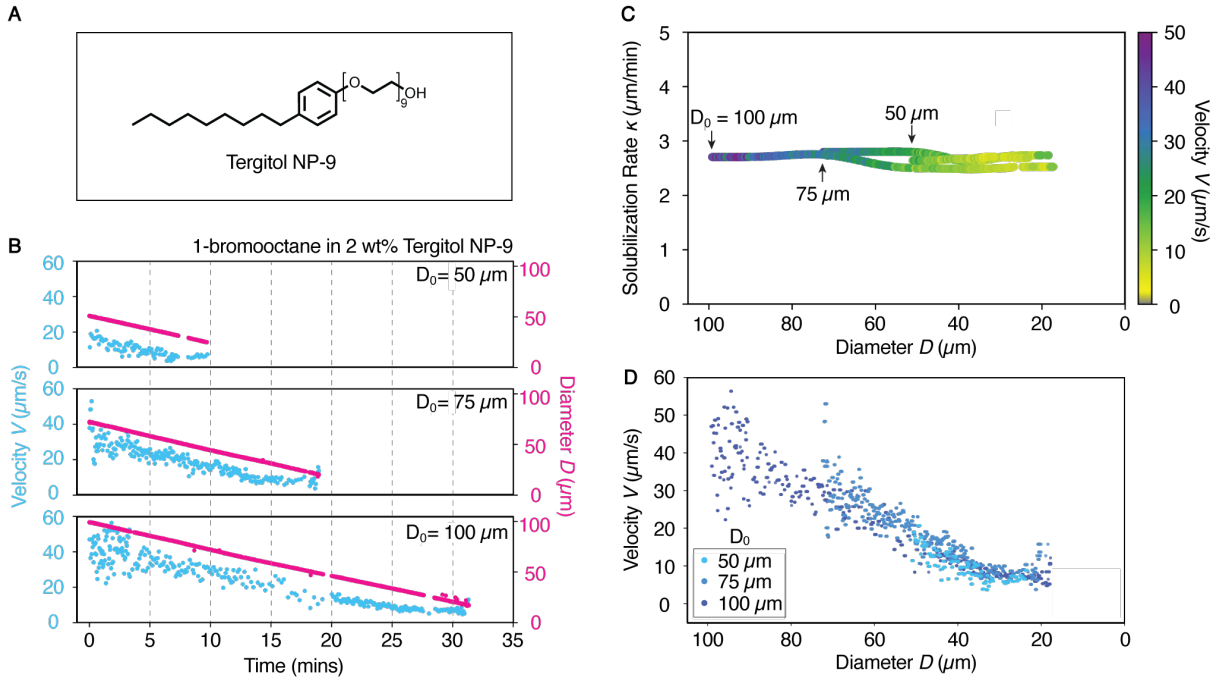

Figure 3. Motility of 1-bromooctane in Tergitol NP-9 nonionic surfactant does not depend on initial diameter. (A) Chemical structure of Tergitol NP-9. The number of ethylene oxide repeats (9) in the headgroup is an average value. **(B)** Time evolution of velocity (blue) and diameter (pink) for 1-bromooctane drops with varying D_0 in 2 wt% Tergitol NP-9. **(C)** Solubilization rate vs diameter with velocity expressed as color at each time point for 1-bromooctane drops in 2 wt% Tergitol NP-9. **(D)** Velocity vs diameter for 1-bromooctane drops in 2 wt% Tergitol NP-9. Data in (B–D) are from the same set of experiments. Representative single droplet trajectories are plotted for clarity; experiments were performed in triplicate and additional data is reported in the SI (**Fig. S3**).

Activity is associated with interfacially-limited solubilization, inactivity with diffusion-limited solubilization. An unresolved question in this work so far is why certain droplets exhibit a constant κ, whereas others display a non-constant solubilization rate, and if this difference is relevant to the mechanisms of droplet motility. Solubilization, at a molecular level, is often described as a two-step process (**Fig. 4A**).[28] First, oil molecules transfer across the interface, a process which has been suggested to impart some level of "interfacial resistance". This step could involve transfer of a single molecule or clusters of molecules (e.g. individual oil molecules, an oil-filled micelle "budding" off the interface, or small aggregates of surfactant and oil). Here, we simply consider this first, interfacial step to be agnostic of the specific pathway by which the oil molecule reaches a micelle; presumably, the precise cause of the resistance is influenced by the chemical structure of the surfactant and oil itself.[24,29] In the second step, oil-filled micelles and oil molecules diffuse away, or are advected away, from the drop's vicinity (a bulk diffusion step). This mass transport problem can be formulated as two resistors in series with resistances R_I and R_B for the interfacial and bulk steps respectively; the total resistance—which determines the solubilization rate—is $R = R_I + R_B$. There are thus two kinetic regimes describing solubilization: an interfacially-limited regime ($R_I \gg R_B$) and a bulk diffusion-limited regime ($R_I \ll R_B$).

Notably, these kinetic regimes differ in how κ depends on D: κ is independent of D under interfacial control, whereas κ increases for smaller D under diffusion control.[24,29] Also, while we expect R_I to be a constant value for given interfacial composition, R_B should change depending on the convective conditions around the droplet. For motile droplets, in both ionic and nonionic surfactants, κ was a larger, relatively constant value independent of D, signaling interfacial control (**Fig. 2,3**). However, for droplets in the non-motile, inactive regime, which we only observed for ionic surfactants, κ was smaller and increased as D decreased, indicative of diffusion limitations. We confirmed that that the solubilization of non-motile drops was diffusion limited by tracking the solubilization rate of a halted, $D_0 = 100$ µm 1-bromooctane drop in 3 wt% SDS under both static and forced convective conditions, finding that the drop with forced convection solubilized faster (**Fig. S4**). Thus, interestingly, drop motility appears to be associated with interfacially-limited solubilization while inactivity associated with diffusion-limited solubilization.

Further, a given droplet can exhibit both active (interfacially limited) and inactive (diffusion limited) regimes at different stages of its lifetime. In the case of droplets which exhibit the stopping behavior in ionic surfactants, drops start in the active regime with interfacially-limited solubilization ($R_I \gg R_B$) where R_B is small because drops are moving quickly (**Fig. 4B**) and convective flow accelerates transport of oil-filled micelles from the drop's vicinity. As the drop's velocity decreases over time, decreased advective transport away from the drop causes an increase in R_B, ultimately leading to a diffusion-limited regime with $R_I \ll R_B$ for inactive (stopped) droplets. This coupling between a drop's motility and its solubilization rate explains the correlated transitions of V and κ observed for the stopping droplets, sketched schematically in **Fig. 4C**. What remained unclear to us was why is this correlated transition dependent upon D_0?

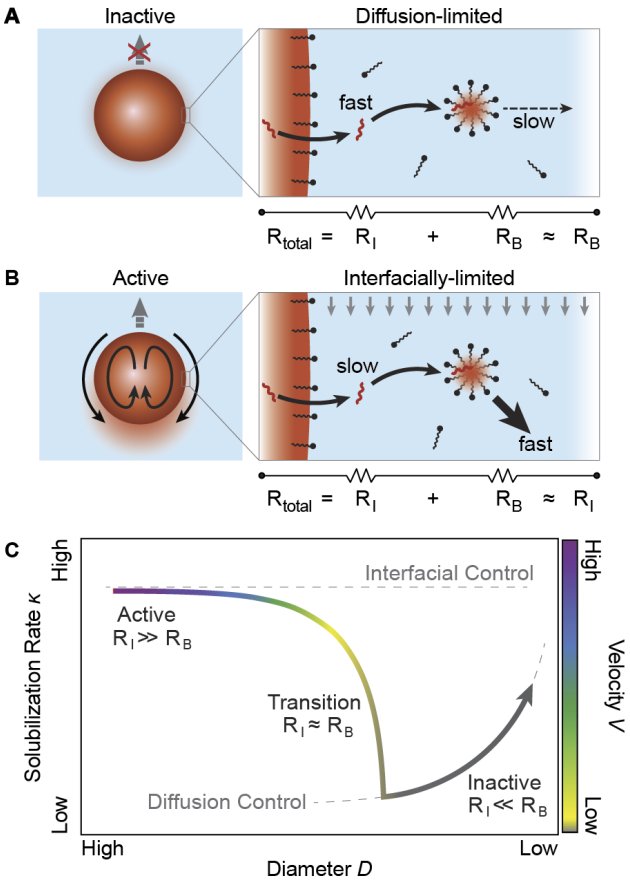

Figure 4. Droplet activity and inactivity appear associated with interfacial and diffusion limited solubilization regimes, respectively. (A) An inactive drop under diffusion-limited solubilization control. Solubilization occurs through two steps: an oil molecule transfers across the interface in a fast process. This could be by molecular transport of oil into water, or potentially by a micellar process, we do not differentiate here. After crossing the interface, the oil-filled micelles and oil molecules diffuse away from the drop's vicinity, which is slow. The solubilization process is represented as two resistors in series with mass transfer resistivities of R_I (interfacial step) and R_B (bulk diffusion step). **(B)** An active drop under interfacially-limited solubilization control. Advection caused by Marangoni flow facilitates a greater flux of filled micelles and oil away from the drop's vicinity, corresponding to a lower R_B compared to the inactive case. **(C)** Schematic of a correlated transition in V and κ for active droplets which experience history dependent halting. The limiting solubilization regimes (interfacial vs diffusion control) are depicted by the dashed lines. Drops start in the active regime with interfacially-limited solubilization ($R_I \gg R_B$). As V decreases, R_B increases due to slower advective transport of filled micelles until $R_I \approx R_B$. As the drop becomes non-motile ($V \to 0$), R_B increases above R_I causing the drop to transition into diffusion-limited solubilization.

To assess whether the solubilization regime and resulting droplet behavior depend on oil chemistry, we examined a series of brominated alkanes with different chain lengths (bromohexane, bromooctane, bromodecane) in 5 wt% SDS with initial diameters of $D_0 = 100 \pm 10\ \mu$m (Fig. S5). While all oils solubilize in SDS, their solubilization kinetics differed markedly. 1-bromohexane droplets were always non-motile, with a solubilization rate that increased as drop diameter decreased, suggesting a diffusion-limited solubilization regime. This behavior could be due to the relatively higher water solubility of the shorter-chain oil, enabling molecular transport (dissolution) of oil into the aqueous phase, rather than via a micellar process[13] and $R_I \ll R_B$. Importantly, the inactivity of the 1-bromohexane droplet, despite an appreciable fast solubilization rate ($-dD/dt = 4.0\ \mu m\ min^{-1}$), indicates that a fast solubilization rate alone is not sufficient to generate Marangoni-driven activity, which is consistent with prior observations.[14,26] In contrast, longer-chain oil 1-bromodecane solubilized the slowest ($-dD/dt = 0.16\ \mu m\ min^{-1}$) and was thus not laterally motile, but it still exhibited weak Marangoni flow at the surface due to symmetry breaking from the substrate[14]; this observation is consistent with solubilization that is interfacially limited, with interfacial transport dominating over bulk diffusion ($R_I \gg R_B$). 1-bromooctane exhibited intermediate behavior, transitioning from interfacially limited solubilization while active to diffusion-limited solubilization while inactive. Together, these results suggest that oil chain length can be used to systematically tune the balance between interfacial and bulk transport resistances, resulting in differences in solubilization kinetics and motility behavior.

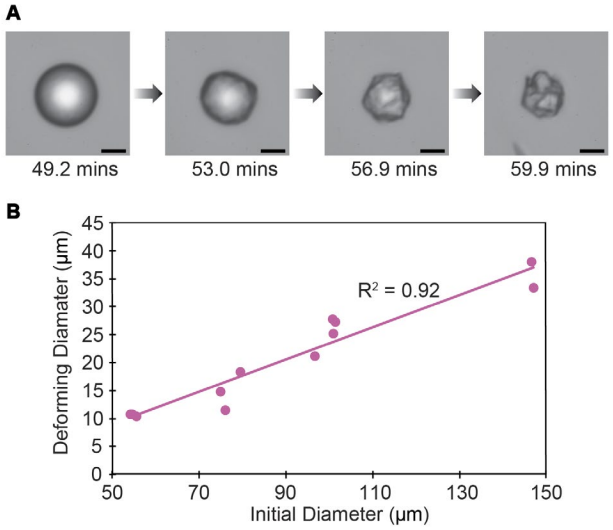

Figure 5. Drops deform at long times after stopping. (A) A $D_0 = 100$ µm 1-bromooctane droplet in 5 wt% SDS undergoes interfacial deformation around 22 minutes after stopping. Scale bar, 10 µm. **(B)** The diameter at which the 1-bromooctane drop interface becomes visually non-spherical in 5 wt% SDS is correlated with the initial diameter. Each point represents the measurement for one droplet.

Droplets often undergo deformation after motility ceases, implying temporal evolution of interfacial composition. While observing 1-bromooctane droplets in 5 wt% SDS and 3 wt% TTAB, we noticed that, if we waited sufficiently long times after the droplet stopped moving (on the order of tens of minutes), drops eventually evolved a non-spherical morphology (Fig. 5A, Video S3). Often, the interface developed wrinkles and eventually collapsed into a crystal-like morphology with flat faces and sharp edges. Even these deformed droplets, however, continued to shrink in size. The deformed drops did not show

birefringence under polarized light microscopy (**Fig. S6**), suggesting that the deformation was likely not due to large-scale molecular ordering or liquid crystal formation within the bulk droplet.[30,31] The deformation was not due to an insoluble impurity in the oil, as further oil purification using column and syringe filtration had no observable effect on deformation (**Fig. S7**) and a wide range of oils exhibited deformation behavior (**Fig. S8**).

Based on the visual onset of interfacial deformation, as well as the temporal variations in the solubilization kinetics / drop motility, we infer that the composition of the drop's interface is gradually changing over time. One possible explanation for the deformation is that surfactant and oil at the drop interface may pack more tightly as the drop's surface area decreases due to solubilization, potentially triggering an interfacial phase transition. This hypothesis is somewhat supported by prior reports of adsorbed surfactants at air-water interfaces undergoing 2D phase transitions when laterally compressed in a Langmuir-Blodgett trough.[32,33] Interestingly, the size at which drops deformed correlated with the droplet's initial diameter (**Fig. 5B**), mirroring the dependence of stopping diameter on initial droplet diameter (**Fig. 2A**).–The correlation in **Fig. 5B** suggests there could be a relationship between the solubilization kinetics and temporal changes in the interfacial composition itself. Since interfacial composition likely impacts interfacial resistance, R_I, and R_I has an impact on velocity, that could be a source of feedback between diameter and velocity that gives rise to memory effects with dependence upon D_0.

Conclusion

We have demonstrated that the non-equilibrium nature of active droplets can manifest as history-dependent motility: in some cases, seemingly identical droplets swim at dramatically different velocities depending on initial conditions. This history-dependence arises from temporal differences in solubilization kinetics where only motile droplets with solubilization rate that decreases over time exhibit history-dependence. Notably, droplet motion is associated only with interfacially limited solubilization while inactivity is associated with a diffusion limited solubilization. We propose that the varying solubilization kinetics might stem from coupling between hydrodynamics and changes in the interfacial composition / an interfacial phase transition, as evidenced by the eventual wrinkling of the droplet surfaces after motion stops.. Further work is needed to probe the interfacial dynamics of these droplets, especially regarding mechanisms of molecular transport across the oil-water interface. This understanding could be applied to examine history-dependence in more complex systems such as emulsions containing non-reciprocal chasing interactions.[26] More broadly, the history-dependence illustrated here introduces new design paradigms for active matter. History-dependence and memory could be desirable for active sensing[34–36] or in biomedical applications[37–39] while controlled studies of collective behaviors might require mitigation of history-dependence to reduce system complexity.[40]

Competing interests. The authors declare no competing interests.

Acknowledgements. The authors acknowledge funding from the Army Research Office grant W911NF-18-1-0414 and the David and Lucile Packard Foundation grant 2019-69664. This work was performed, in part, at the Center for Integrated Nanotechnologies, an Office of Science User Facility operated for the U.S. Department of Energy (DOE) Office of Science. Sandia National Laboratories is a multimission laboratory managed and operated by National Technology & Engineering Solutions of Sandia, LLC, a wholly owned subsidiary of Honeywell International, NC., for the U.S. DOE's National Nuclear Security Administration under contract DE-NA-0003525. The views expressed in the article do not necessarily represent the views of the U.S. DOE or the United States Government.

References

(1) Jambon-Puillet, E.; Testa, A.; Lorenz, C.; Style, R. W.; Rebane, A. A.; Dufresne, E. R. Phase-Separated Droplets Swim to Their Dissolution. *Nat. Commun.* **2024**, *15* (1), 3919. https://doi.org/10.1101/2023.07.18.549556.

(2) Nsamela, A.; Garcia Zintzun, A. I.; Montenegro-Johnson, T. D.; Simmchen, J. Colloidal Active Matter Mimics the Behavior of Biological Microorganisms—An Overview. *Small* **2023**, *19* (13), 2202685. https://doi.org/10.1002/smll.202202685.

(3) de Visser, P. J.; Karagrigoriou, D.; Nguindjel, A. D. C.; Korevaar, P. A. Quorum Sensing in Emulsion Droplet Swarms Driven by a Surfactant Competition System. Advanced Science **2024**, *11* (30). https://doi.org/10.1002/advs.202307919.

(4) Kasuo, Y.; Kitahata, H.; Koyano, Y.; Takinoue, M.; Asakura, K.; Banno, T. Start of Micrometer-Sized Oil Droplet Motion through Generation of Surfactants. *Langmuir* **2019**, *35* (41), 13351–13355. https://doi.org/10.1021/acs.langmuir.9b01722.

(5) Hanczyc, M. M. Droplets: Unconventional Protocell Model with Life-Like Dynamics and Room to Grow. *Life* **2014**, *4* (4), 1038–1049. https://doi.org/10.3390/life4041038.

(6) Silvera Batista, C. A.; Wang, K.; Blake, H.; Nwosu-Madueke, V.; Marbach, S. Artificial Chemotaxis under Electrodiffusiophoresis. *J Colloid Interface Sci* **2025**, *677*, 171–180. https://doi.org/10.1016/j.jcis.2024.08.004.

(7) Maass, C. C.; Michelin, S.; Zarzar, L. D. Self-Propelling Droplets. *Annu. Rev. Condens. Matter Phys.* **2020**, *11*, 171–193. https://doi.org/10.1146/annurev-conmatphys-031119-050730.

(9) Birrer, S.; Cheon, S. I.; Zarzar, L. D. We the Droplets: A Constitutional Approach to Active and Self-Propelled Emulsions. *Curr. Opin. Colloid Interface Sci.* **2022**, *61*, 101623. https://doi.org/10.1016/j.cocis.2022.101623.

(10) Michelin, S. Self-Propulsion of Chemically-Active Droplets. *Annu. Rev. Fluid Mech.* **2022**, *54*, 321–345. https://doi.org/10.1146/annurev-fluid-120720-012204.

(11) Izri, Z.; Van Der Linden, M. N.; Michelin, S.; Dauchot, O. Self-Propulsion of Pure Water Droplets by Spontaneous Marangoni-Stress-Driven Motion. *Phys. Rev. Lett.* **2014**, *113* (24), 248302. https://doi.org/10.1103/PhysRevLett.113.248302.

(12) Jin, C.; Krüger, C.; Maass, C. C. Chemotaxis and Autochemotaxis of Self-Propelling Droplet Swimmers. *Proc. Natl. Acad. Sci. U.S.A.* **2017**, *114* (20), 5089–5094. https://doi.org/10.1073/pnas.1619783114.

(13) D Dwivedi, P.; Si, B. R.; Pillai, D.; Mangal, R. Solute Induced Jittery Motion of Self-Propelled Droplets. *Phys. Fluids* **2021**, *33* (2), 022103. https://doi.org/10.1063/5.0038716.

(14) Wentworth, C. M.; Castonguay, A. C.; Moerman, P. G.; Meredith, C. H.; Balaj, R. V.; Cheon, S. I.; Zarzar, L. D. Chemically Tuning Attractive and Repulsive Interactions between Solubilizing Oil Droplets. *Angew. Chem., Int. Ed.* **2022**, *61* (32), e202204510. https://doi.org/10.1002/anie.202204510.

(15) Herminghaus, S.; Maass, C. C.; Krüger, C.; Thutupalli, S.; Goehring, L.; Bahr, C. Interfacial Mechanisms in Active Emulsions. *Soft Matter* **2014**, *10* (36), 7008–7022. https://doi.org/10.1039/c4sm00550c.

(16) Kim, K. E.; Balaj, R. V.; Zarzar, L. D. Chemical Programming of Solubilizing, Nonequilibrium Active Droplets. *Acc Chem Res* **2024**, *57* (16), 2372–2382. https://doi.org/10.1021/acs.accounts.4c00299.

(17) Morozov, M. Adsorption Inhibition by Swollen Micelles May Cause Multistability in Active Bowick, M. J.; Fakhri, N.; Marchetti, M. C.; Ramaswamy, S. Symmetry, Thermodynamics, and Topology in Active Matter. *Phys. Rev. X* **2022**, *12* (1), 010501. https://doi.org/10.1039/d0sm00662a.

(18) Moerman, P. G.; Moyses, H. W.; Van Der Wee, E. B.; Grier, D. G.; Van Blaaderen, A.; Kegel, W. K.; Groenewold, J.; Brujic, J. Solute-Mediated Interactions between Active Droplets. *Phys. Rev. E* **2017**, *96* (3), 032607. https://doi.org/10.1103/PhysRevE.96.032607.

(19) Lancia, F.; Yamamoto, T.; Ryabchun, A.; Yamaguchi, T.; Sano, M.; Katsonis, N. Reorientation Behavior in the Helical Motility of Light-Responsive Spiral Droplets. *Nat. Commun.* **2019**, *10* (1), 5238. https://doi.org/10.1038/s41467-019-13201-6.

(20) Atkins, P. W.; de Paula, J. *Physical Chemistry*, 11th ed.; Oxford University Press: Oxford, **2017**.

(21) Sollich, P. Rheological Constitutive Equation for a Model of Soft Glassy Materials. *Phys. Rev. E* **1998**, *58* (1), 738–759.

(22) Sollich, P.; Lequeux, F.; Hébraud, P.; Cates, M. E. Rheology of Soft Glassy Materials. *Phys. Rev. Lett.* **1997**, *78* (10), 2020–2023.

(23) Ueno, N.; Banno, T.; Asami, A.; Kazayama, Y.; Morimoto, Y.; Osaki, T.; Takeuchi, S.; Kitahata, H.; Toyota, T. Self-Propelled Motion of Monodisperse Underwater Oil Droplets Formed by a Microfluidic Device. *Langmuir* **2017**, *33* (22), 5393–5397. https://doi.org/10.1021/acs.langmuir.7b00092.

(24) Todorov, P. D.; Kralchevsky, P. A.; Denkov, N. D.; Broze, G.; Mehreteab, A. Kinetics of Solubilization of N-Decane and Benzene by Micellar Solutions of Sodium Dodecyl Sulfate. *J. Colloid Interface Sci.* **2002**, *245* (2), 371–382. https://doi.org/10.1006/jcis.2001.8031.

(25) Michelin, S.; Lauga, E.; Bartolo, D. Spontaneous Autophoretic Motion of Isotropic Particles. *Phys. Fluids* **2013**, *25* (6), 061701. https://doi.org/10.1063/1.4810749.

(26) Meredith, C. H.; Moerman, P. G.; Groenewold, J.; Chiu, Y. J.; Kegel, W. K.; van Blaaderen, A.; Zarzar, L. D. Predator–Prey Interactions between Droplets Driven by Non-Reciprocal Oil Exchange. *Nat. Chem.* **2020**, *12* (12), 1136–1142. https://doi.org/10.1038/s41557-020-00575-0.

(27) Castonguay, A. C.; Kailasham, R.; Wentworth, C. M.; Meredith, C. H.; Khair, A. S.; Zarzar, L. D. Gravitational Settling of Active Droplet. *Phys Rev E* **2023**, *107* (2). https://doi.org/10.1103/physreve.107.024608.

(28) Shah, R.; Neogi, P. Interfacial Resistance in Solubilization Kinetics. *J. Colloid Interface Sci.* **2002**, *253* (2), 443–454. https://doi.org/10.1006/jcis.2002.8449.

(29) Peña, A. A.; Miller, C. A. Solubilization Rates of Oils in Surfactant Solutions and Their Relationship to Mass Transport in Emulsions. *Adv. Colloid Interface Sci.* **2006**, *123–126*, 241–257. https://doi.org/10.1016/j.cis.2006.05.005.

(30) Denkov, N.; Tcholakova, S.; Lesov, I.; Cholakova, D.; Smoukov, S. K. Self-Shaping of Oil Droplets via the Formation of Intermediate Rotator Phases upon Cooling. *Nature* **2015**, *528* (7582), 392–395. https://doi.org/10.1038/nature16189.

(31) Cholakova, D.; Glushkova, D.; Valkova, Z.; Tsibranska-Gyoreva, S.; Tsvetkova, K.; Tcholakova, S.; Denkov, N. Rotator Phases in Hexadecane Emulsion Drops Revealed by X-Ray Synchrotron Techniques. *J. Colloid Interface Sci.* **2021**, *604*, 260–271. https://doi.org/10.1016/j.jcis.2021.06.122.

(32) Hossain, M. M.; Suzuki, T.; Kato, T. Phases and Phase Transitions in Gibbs Monolayers of an Alkyl Phosphate Surfactant. *J. Colloid Interface Sci.* **2005**, *288* (2), 342–349. https://doi.org/10.1016/j.jcis.2005.03.006.

(33) Hossain, M. M.; Iimura, K. I.; Kato, T. How Many Phases and Phase Transitions Do Exist in Gibbs Adsorption Layers at the Air-Water Interface? *J. Colloid Interface Sci.* **2007**, *306* (2), 391–397. https://doi.org/10.1016/j.jcis.2006.10.071.

(34) Zarzar, L. D.; Kalow, J. A.; He, X.; Walish, J. J.; Swager, T. M. Optical Visualization and Quantification of Enzyme Activity Using Dynamic Droplet Lenses. *Proc. Natl. Acad. Sci. U.S.A.* **2017**, *114* (15), 3821–3825. https://doi.org/10.1073/pnas.1618807114.

(35) Zeininger, L. Responsive Janus Droplets as Modular Sensory Layers for the Optical Detection of Bacteria. *Anal. Bioanal. Chem.* **2023**, *415* (21), 5205–5219. https://doi.org/10.1007/s00216-023-04838-w.

(36) Mukherjee, F.; Shi, A.; Wang, X.; You, F.; Abbott, N. L. Liquid Crystals as Multifunctional Interfaces for Trapping and Characterizing Colloidal Microplastics. *Small* **2023**, *19* (23), 2207802. https://doi.org/10.1002/smll.202207802.

(37) Xu, C.; Shi, H.; Tan, Z.; Zheng, Y.; Xu, W.; Dan, Z.; Liao, J.; Dai, Z.; Zhao, Y. Generation, Manipulation, Detection and Biomedical Applications of Magnetic Droplets in Microfluidic Chips. *Analyst* **2024**, *149* (10), 5591–5616. https://doi.org/10.1039/d4an01175a.

(38) Ngocho, K.; Yang, X.; Wang, Z.; Hu, C.; Yang, X.; Shi, H.; Wang, K.; Liu, J. Synthetic Cells from Droplet-Based Microfluidics for Biosensing and Biomedical Applications. *Small* **2024**, *20* (33), 2400086. https://doi.org/10.1002/smll.202400086.

(39) Liu, D.; Sun, M.; Zhang, J.; Hu, R.; Fu, W.; Xuanyuan, T.; Liu, W. Single-Cell Droplet Microfluidics for Biomedical Applications. *Analyst* **2022**, *147* (8), 2294–2316. https://doi.org/10.1039/d1an02321g.

(40) Krüger, C.; Bahr, C.; Herminghaus, S.; Maass, C. C. Dimensionality Matters in the Collective Behaviour of Active Emulsions. *Eur. Phys. J. E* **2016**, *39* (6), 64. https://doi.org/10.1140/epje/i2016-16064-y.